Australian Government
Department of Defence
Defence Science and
Technology Organisation

3D Self-Localisation from Angle of Arrival Measurements

*Jijoong Kim and Hatem Hmam**

Weapons Systems Division
***Electronic Warfare and Radar Division**
Defence Science and Technology Organisation

DSTO-TR-2278

ABSTRACT

We propose a 3D self-localisation method that uses 3D angle of arrival (AOA) information (ie., azimuth and elevation measurements) from landmarks. The formulation is based on minimising the collinearity error between the estimated line of sight (LOS) to the landmark and the measured AOA. This method runs in two parts – initial estimation of the vehicle azimuth and position assuming the vehicle has no tilt, and iterative 3D pose estimation based on a small angle approximation approach. Simulation study indicates that this method is efficient, requiring a small number of iterations, globally convergent and robust.

Published by

Weapons Systems Division
DSTO Defence Science and Technology Organisation
PO Box 1500
Edinburgh South Australia 5111 Australia

Telephone: (08) 8259 5555
Fax: (08) 8259 6567

AR-014-502
April 2009

APPROVED FOR PUBLIC RELEASE

3D Self-Localisation from Angle of Arrival Measurements

Executive Summary

In this report, we introduce a 3D self-localisation method that uses three-dimensional angle of arrival (AOA) information (i.e. azimuth and elevation measurements) from landmarks. We assume here that such measurements are available, even though in practice they need to be processed from the onboard sensors such as cameras or RF receivers.

This work is a follow on to our previous study on 2D localisation where the altitude and the tilt angle of the vehicle were not relevant. However, in many applications the vehicle on-board sensor may be tilted making bearing measurements erroneous. In these situations the localisation problem has to be formulated in six-degrees of freedom (i.e. 3 DOF for sensor position and 3 DOF for sensor orientation).

The formulation is based on minimising the collinearity error between the estimated line of sight (LOS) and the measured AOA. Using such error metric, we arrive at an iterative algorithm that runs in two parts: initial estimation of position and azimuth assuming zero tilt, followed by iterative orientation and position updates using small angle approximation approach.

The proposed method is evaluated against a benchmark known as the *orthogonal iteration* which is known to be accurate, globally convergent, and efficient. The experimental results indicate that the proposed method is more accurate than the benchmark. The proposed method is also efficient requiring a small number of iterations and appears to be globally convergent.

Authors

Jijoong Kim
Weapons Systems Division

Jijoong Kim received a B.E. (Hons) in Electrical and Electronic Engineering and M.EngSc. both from the University of Adelaide in 1993 and 1995 respectively. He was a research assistant at the EE department of the University of Adelaide for months, and then joined DSTO in November 1995. During his employment with DSTO, he completed a PhD in Image Processing and Computer Vision from the University of Wollongong in 2006. Since 1995, he has been with the Guidance and Control Group. His research interests include: Missile Guidance, Optimal Control, Navigation, and Computer Vision.

Hatem Hmam
Electronic Warfare and Radar Division

Hatem Hmam received his Ph.D. degree in Electrical Engineering from University of Cincinnati, Ohio, USA, in 1992. He then pursued post-doctoral research in jet engine control at University of Colorado, Boulder, and signal processing at Queensland University of Technology, Brisbane. He joined DSTO in 1996 and worked in WSD and EWRD Divisions. He is currently a member of Distributed Electronic Warfare group where he is developing and implementing passive localisation techniques of RF emitters.

Contents

ACRONYMS

AOA	Angle of Arrival
AIPE	Angle Increment and Position Estimation
AO	Absolution Orientation
AZIPE	Azimuth and Position Estimation
CRLB	Cramer Rao Lower Bound
GPS	Global Positioning System
LOS	Line of Sight
MLE	Maximum Likelihood Estimation/Estimator
OI	Orthogonal Iteration
RF	Radio Frequency
RMS	Root Mean Square
SVD	Singular Vector Decomposition
UAV	Unmanned Aerial Vehicle
UGV	Unmanned Ground Vehicle
uLOS	Unit Line of Sight

SYMBOLS

(α_i, β_i)	azimuth and elevation angle measurements to the i^{th} landmark
$x, \mathbf{x}, \mathbf{X}$	scalar, vector and matrix expressions for parameter x
$\mathbf{p}_i$	i^{th} landmark position in the reference frame
$\mathbf{p}_{vehicle}$	vehicle position in the reference frame
$\mathbf{q}_i$	i^{th} landmark position in the translated reference frame
$\mathbf{b}$	vehicle position in the translated reference frame
d_i	distance between $\mathbf{q}_i$ and the estimated vehicle position, $\hat{\mathbf{b}}$
n	number of landmarks
$\mathbf{R}$	rotation matrix from the reference frame to the body frame
$\mathbf{t}$	translation vector $(\mathbf{t} = -\mathbf{Rb})$
$\mathbf{v}_i$	uLOS measurement vector to i^{th} landmark
$\mathbf{V}_i$	projection matrix $(= \mathbf{v}_i \mathbf{v}_i^T)$
(ϕ, θ, ψ)	roll, pitch and yaw angles of the vehicle
$\mathbf{e}$	vector to be estimated
E	quadratic cost function
σ	standard deviation
σ_x^2	variance of variable x
$\mathbf{N}$	measurement error covariance matrix
$\mathbf{P}$	estimation error covariance matrix

1. Introduction

The capabilities that unmanned robotic vehicles provide are expected to revolutionise the way combat operations are conducted. The UAV or UGV will reduce the risk to soldiers in hazardous situations, and alleviate the human workload and manpower requirements. Possible applications include: search and rescue (in land and sea), surveillance of military bases or nuclear sites, demining activities, underwater construction and mapping, agriculture, logistics in battle fields.

One of the key components in autonomous functionality is localisation, which is the process of determining its own position and orientation using onboard sensors or radio links. We are particularly interested in *landmark-based localisation* which is attractive in a controlled environment where the landmarks can be precisely located.

In open outdoor environments, differential GPS systems can provide precise position information. However, there are situations where GPS is not adequate such as indoor, underwater, extraterrestrial or urban environments, because of signal blockage and multipath interferences. Furthermore, for stand-alone GPS systems, the position accuracy may not be sufficient. In military context, GPS receivers at low altitudes are more susceptible to jamming or spoofing from the adversary. A simple alternative would be odometry or inertial navigation system (INS). However, both are subject to build-up of error with time, and often require an external aid.

In this report, we introduce a 3D self-localisation method that uses 3D angle of arrival (AOA) measurements (i.e. azimuth and elevation) from surrounding landmarks. We assume that the AOA measurements are available, even though in practice they need to be collected from the onboard sensors such as cameras or RF receivers.

This work is an extension of our previous report on 2D localisation [4] where the altitude and the tilt angle were not considered (assumed zero). In practice, vehicles (especially the airborne vehicles) can be tilted at times, adding errors to the bearing-only measurements. In these situations the localisation problem has to be formulated in six-degrees of freedom (i.e. 3 DOF for sensor position and 3 DOF for sensor orientation).

We formulate the localisation problem as one of minimising the collinearity error between the estimated line of sight (LOS) and the measured AOA, as shown in Figure 1. Using such error metric, we arrive at an iterative algorithm that runs in two parts: initial estimation of position and azimuth assuming zero tilt, followed by iterative orientation and position updates using small angle approximation approach. This method is efficient requiring a small number of iterations and is shown to be globally convergent and robust.

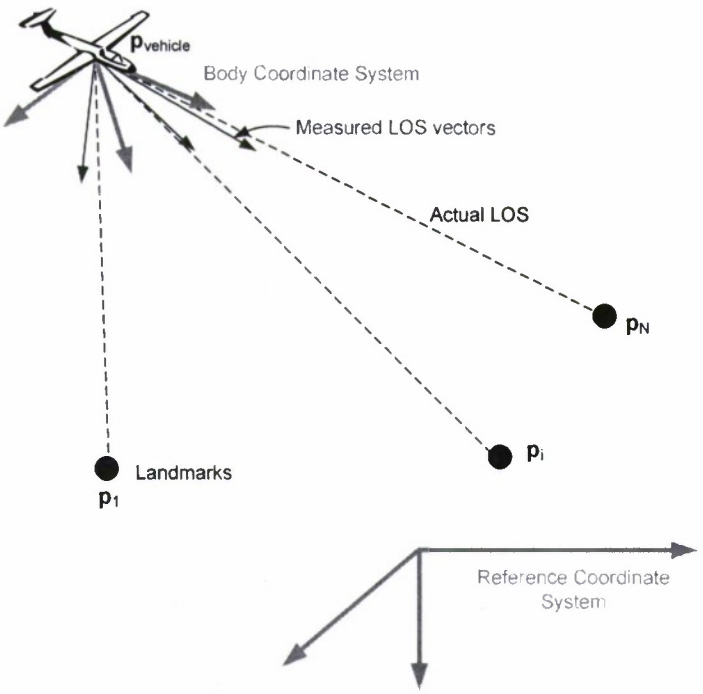

Figure 1: Illustration of UAV taking noisy AOA measurements from landmarks in order to estimate its position and orientation

This report is organised as follows: Section 2 describes the formulation of the proposed method and re-visits an existing method which will be used as a benchmark. In Section 3, simulation results and performance comparisons with the benchmark are given. Finally, Section 4 summaries and concludes the study.

2. Problem Formulations

2.1 Optimisation of Translation Vector

The points, $\mathbf{p}_i$, in Figure 1, are landmark positions given in the external reference frame. We first move them so that their mean coincides with the new origin. The translated landmark positions are given by

$$\mathbf{q}_i = \mathbf{p}_i - \bar{\mathbf{p}} \text{ where } \bar{\mathbf{p}} = \frac{1}{n}\sum_{j=1}^{n}\mathbf{p}_j . \quad (1)$$

Note that $\bar{\mathbf{q}} = \mathbf{0}$.

In the translated frame, we define $\mathbf{b}$ as the vehicle position, and $\mathbf{v}_i$ as the unit line of sight (uLOS) vector from $\mathbf{b}$ to $\mathbf{q}_i$, expressed in body frame (see Figure 2).

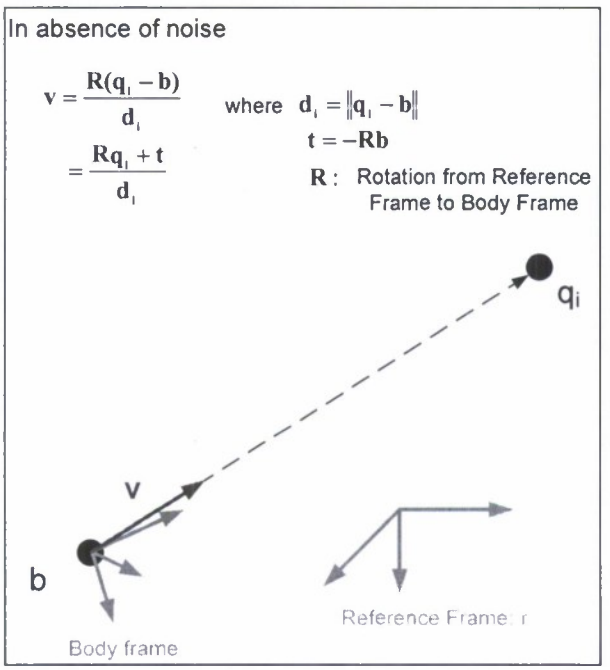

Figure 2: Definition of unit line of sight vector $\mathbf{v}$*, and translation vector* $\mathbf{t}$*. Note* $\mathbf{v}$ *is expressed in the sensor (body) frame.*

In the absence of measurement errors, we have the following relationship,

$$\mathbf{v}_i = \frac{\mathbf{R}(\mathbf{q}_i - \mathbf{b})}{d_i} = \frac{\mathbf{R}\mathbf{q}_i + \mathbf{t}}{d_i} \tag{2}$$

where

- d_i is the distance between $\mathbf{q}_i$ and the estimated vehicle position, $\mathbf{b}$.
- $\mathbf{R}$ is the rotation matrix from the reference frame to the body frame, and
- $\mathbf{t}$ is the translation vector $(\mathbf{t} = -\mathbf{R}\mathbf{b})$.

In the presence of measurement errors, $\mathbf{v}_i$ is no longer equal to $\frac{\mathbf{R}\mathbf{q}_i + \mathbf{t}}{d_i}$, and the objective becomes to minimise the following cost function,

$$E(\mathbf{R},\mathbf{t}) = \sum_{i=1}^{n} \left\| \mathbf{v}_i \times \left[\frac{\mathbf{R}\mathbf{q}_i + \mathbf{t}}{d_i} \right] \right\|^2 \tag{3}$$

where $\mathbf{v}_i$ is the unit pointing vector along the *measured* azimuth β_i and elevation α_i to the i^{th} landmark. This error metric is a measure of the collinearity between the measured and estimated uLOS vectors.

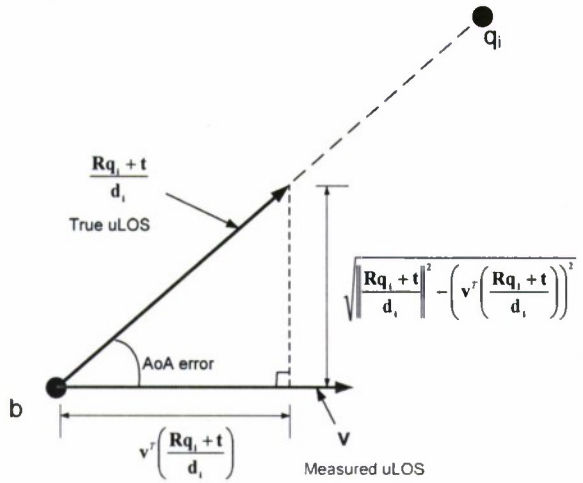

Figure 3: Definition of the error metric as the collinearity of estimated and measured uLOS vectors

Examining Figure 3, the error given by (3) can also be expressed as

$$E(\mathbf{R},\mathbf{t}) = \sum_{i=1}^{n} \left\| \frac{\mathbf{Rq}_i + \mathbf{t}}{d_i} \right\|^2 - \left(\mathbf{v}_i^T \left[\frac{\mathbf{Rq}_i + \mathbf{t}}{d_i} \right] \right)^2 \tag{4}$$

If we let $\mathbf{V}_i = \mathbf{v}_i \mathbf{v}_i^T$, then the optimal translation vector, $\mathbf{t}$, can be obtained by solving the equation below.

$$\nabla_{\mathbf{t}} E(\mathbf{R},\mathbf{t}) = \sum_{i=1}^{n} \frac{1}{d_i^2} \{ 2(\mathbf{I} - \mathbf{V}_i)\mathbf{t} + 2(\mathbf{I} - \mathbf{V}_i)\mathbf{Rq}_i \} = \mathbf{0} \tag{5}$$

If we let

$$\mathbf{\Lambda}_i = \frac{(\mathbf{I} - \mathbf{V}_i)}{d_i^2}, \ (3 \times 3) \tag{6}$$

Then (5) becomes

$$(\sum_{i=1}^{n} \mathbf{\Lambda}_i)\mathbf{t} + \sum_{i=1}^{n} \mathbf{\Lambda}_i \mathbf{Rq}_i = \mathbf{0} \tag{7}$$

By rearranging (7), we obtain $\mathbf{t}_{opt}$ as below,

$$\mathbf{t}_{opt} = -\mathbf{\Lambda}^{-1} \sum_{i=1}^{n} \mathbf{\Lambda}_i \mathbf{Rq}_i \ \text{ where } \ \mathbf{\Lambda} = \sum_{i=1}^{n} \mathbf{\Lambda}_i \ . \tag{8}$$

2.2 Azimuth and Position Estimation (AZIPE)

The rotation terms (ie., roll, pitch, and azimuth) are expressed as sums and products of trigonometric functions in $\mathbf{R}$, making the objective function in Equation (4) highly non-linear. Finding the closed-form solution for all three angles is very challenging.

To simplify the approach, we assume that the roll (ϕ) and pitch (θ) are known, and try to find the optimal azimuth (ψ). The rotation from the reference to body frames is given as

$$\mathbf{R} = \begin{bmatrix} h\cos\psi & h\sin\psi & -a \\ k\cos\psi - l\sin\psi & l\cos\psi + k\sin\psi & b \\ u\cos\psi + v\sin\psi & -v\cos\psi + u\sin\psi & c \end{bmatrix} \tag{9}$$

where

$h = \cos\theta,\ k = \sin\phi\sin\theta,\ l = \cos\phi,\ u = \cos\phi\sin\theta$
$v = \sin\phi,\ a = \sin\theta,\ b = \sin\phi\cos\theta,\ c = \cos\phi\cos\theta$

We define e the vector to be estimated as

$$\mathbf{e} = [\cos\psi, \sin\psi]^T \tag{10}$$

Then $\mathbf{Rq}_i$ in Equation (8) can be expressed as linear equation of e.

$$\mathbf{Rq}_i = \mathbf{Q}_i\mathbf{e} + \mathbf{s}_i \tag{11}$$

$$\text{where } \mathbf{q}_i = \begin{bmatrix} q_{ix} \\ q_{iy} \\ q_{iz} \end{bmatrix},\ \mathbf{Q}_i = \begin{bmatrix} hq_{ix} & hq_{iy} \\ kq_{ix} + lq_{iy} & -lq_{ix} + kq_{iy} \\ uq_{ix} - vq_{iy} & vq_{ix} + uq_{iy} \end{bmatrix} \text{ and } \mathbf{s}_i = q_{iz}\begin{bmatrix} -a \\ b \\ c \end{bmatrix} \tag{12}$$

Therefore $\mathbf{t}_{opt}$ in (8) becomes

$$\begin{aligned} \mathbf{t}_{opt}(\mathbf{e}) &= -\mathbf{\Lambda}^{-1}\sum_{i=1}^{n}\mathbf{\Lambda}_i(\mathbf{Q}_i\mathbf{e} + \mathbf{s}_i) \\ &= \left(-\mathbf{\Lambda}^{-1}\sum_{i=1}^{n}\mathbf{\Lambda}_i\mathbf{Q}_i\right)\mathbf{e} - \mathbf{\Lambda}^{-1}\sum_{i=1}^{n}\mathbf{\Lambda}_i\mathbf{s}_i \end{aligned}$$

$$\mathbf{t}_{opt}(\mathbf{e}) = \mathbf{F}\mathbf{e} + \mathbf{w} \tag{13}$$

$$\text{where } \mathbf{F} = -\mathbf{\Lambda}^{-1}\sum_{i=1}^{n}\mathbf{\Lambda}_i\mathbf{Q}_i \text{ and } \mathbf{w} = -\mathbf{\Lambda}^{-1}\sum_{i=1}^{n}\mathbf{\Lambda}_i\mathbf{s}_i \tag{14}$$

Finally, from (11) and (13), we have an expression for $\mathbf{Rq}_i + \mathbf{t}_{opt}$ as

$$\mathbf{Rq}_i + \mathbf{t}_{opt} = \mathbf{G}_i\mathbf{e} + \mathbf{g}_i \tag{15}$$

where $\mathbf{G}_i = \mathbf{F} + \mathbf{Q}_i$ and $\mathbf{g}_i = \mathbf{w} + \mathbf{s}_i$. (16)

After, substituting (16) into (4) (see Appendix B for details), we arrive at the following quadratic cost function

$$E(\mathbf{e}) = \mathbf{e}^T \mathbf{M} \mathbf{e} + 2\mathbf{m}^T \mathbf{e} + d \tag{17}$$

where

$$\mathbf{M} = \sum_{i=1}^{n} \mathbf{G}_i^T \mathbf{\Lambda}_i \mathbf{G}_i \quad (2\times 2) \tag{18}$$

$$\mathbf{m} = \sum_{i=1}^{n} \mathbf{G}_i^T \mathbf{\Lambda}_i \mathbf{g}_i \quad (2\times 1) \text{ and} \tag{19}$$

$$d = \sum_{i=1}^{n} \mathbf{g}_i^T \mathbf{\Lambda}_i \mathbf{g}_i \tag{20}$$

We substitute (10) into (17) and obtain,

$$\begin{aligned} E(\psi) &= [\cos\psi \ \sin\psi] \begin{bmatrix} M_{11} & M_{12} \\ M_{12} & M_{22} \end{bmatrix} \begin{bmatrix} \cos\psi \\ \sin\psi \end{bmatrix} + 2m_1 \cos\psi + 2m_2 \sin\psi + d \\ &= (M_{11} - M_{22}) \cos^2\psi + 2M_{12} \cos\psi \sin\psi + 2m_1 \cos\psi + 2m_2 \sin\psi + M_{22} + d \\ &= A\cos^2\psi + B\cos\psi\sin\psi + C\cos\psi + S\sin\psi + D. \end{aligned} \tag{21}$$

The optimal angle is obtained by differentiating E with respect to ψ and setting the derivative to zero as,

$$\frac{dE}{d\psi} = -2A\cos\psi\sin\psi + 2B\cos^2\psi - B - C\sin\psi + S\cos\psi = 0 \tag{22}$$

This leads to

$$2B\cos^2\psi + S\cos\psi - B = 2A\cos\psi\sin\psi + C\sin\psi \ \text{q} \tag{23}$$

which after squaring and rearranging, results in

$$A_4 x^4 + A_3 x^3 + A_2 x^2 + A_1 x + A_0 = 0 \tag{24}$$

where $x = \cos\psi$ and

$$\begin{aligned} A_4 &= 4\left(A^2 + B^2\right) \\ A_3 &= 4\left(AC + BS\right) \\ A_2 &= S^2 + C^2 - A_4 \\ A_1 &= -4AC - 2BS \\ A_0 &= B^2 - C^2 \end{aligned}$$

Solving this quartic equation may, in theory, yield up to 4 real solutions. However, only those satisfying $-1 \le x \le 1$ are acceptable. The azimuth is given as $\psi = \cos^{-1}(x)$ for each solution x, and we choose the one associated with the smallest $E(\psi)$.

We put ψ_{opt} into Equation (9) to obtain the optimal rotation, $\mathbf{R}$, and the vehicle position is then obtained as

$$\mathbf{p}_{\text{vehicle}} = -\mathbf{R}^T \mathbf{t}_{\text{op}} + \overline{\mathbf{p}} . \tag{25}$$

This solution is accurate if the initial tilt angles are known or accurately guessed. Often the exact tilt angles are unknown but small. We therefore assume they are zero, solve (24), and obtain an approximate solution for the vehicle's position and orientation. This approximate solution can be refined as explained in the next subsection. But before moving to the next subsection, we note that once an estimated vehicle position is computed, then approximate values for the parameters, d_i, in (2) can be obtained as $\|\mathbf{p}_{\text{vehicle}} - \mathbf{p}_i\|$.

2.3 Angle Increments and Position Estimation (AIPE)

Once the AZIPE algorithm is executed, we are given initial orientation estimates for ϕ_0, θ_0 and ψ_0. Often these estimates are very close to the optimal solution. To refine their estimates, we perturb them as $\phi = \phi_0 + \delta\phi$, $\theta = \theta_0 + \delta\theta$, and $\psi = \psi_0 + \delta\psi$, and re-derive the objective function (4) using the new small angle variables, $(\delta\phi, \delta\theta, \delta\psi)$.

The rotation matrix by definition is given as

$$\mathbf{R} = \begin{bmatrix} \cos\theta\cos\psi & \cos\theta\sin\psi & -\sin\theta \\ -\cos\phi\sin\psi + \sin\phi\sin\theta\cos\psi & \cos\phi\cos\psi + \sin\phi\sin\theta\sin\psi & \cos\theta\sin\varphi \\ \sin\phi\sin\psi + \cos\phi\cos\psi\sin\theta & -\cos\psi\sin\phi + \sin\theta\sin\psi\cos\phi & \cos\phi\cos\theta \end{bmatrix} \tag{26}$$

By substituting $\phi = \phi_0 + \delta\phi$, $\theta = \theta_0 + \delta\theta$, and $\psi = \psi_0 + \delta\psi$ into Equation (26), expanding and collecting the first order terms, then each element in R can be expressed as a linear function of the incremental terms $\{\delta\phi, \delta\theta, \delta\psi\}$.

$$\mathbf{R} \cong \begin{bmatrix} c1 & c2 & c3 \\ c4 & c5 & c6 \\ c7 & c8 & c9 \end{bmatrix} \tag{27}$$

where $ci = ci_0 + ci_1\delta\phi + ci_2\delta\theta + ci_3\delta\psi \quad , i = 1 \ldots 9$. The details of elements ($c1$, …, $c9$) are given in Appendix B

Again we need to re-express $\mathbf{Rq}_i$ from Equation (8) in the form of $\mathbf{Q}_i\mathbf{e} + \mathbf{s}_i$.

$$\mathbf{Rq}_i = \begin{bmatrix} c1 & c2 & c3 \\ c4 & c5 & c6 \\ c7 & c8 & c9 \end{bmatrix} \begin{bmatrix} q_{ix} \\ q_{iy} \\ q_{iz} \end{bmatrix}$$

$$= \begin{bmatrix} (cl_0 q_{ix} + c2_0 q_{iy} + c3_0 q_{iz}) + (cl_1 q_{ix} + c2_1 q_{iy} + c3_1 q_{iz})\Delta\phi + (cl_2 q_{ix} + c2_2 q_{iy} + c3_2 q_{iz})\Delta\theta + (cl_3 q_{ix} + c2_3 q_{iy} + c3_3 q_{iz})\Delta\psi \\ (c4_0 q_{ix} + c5_0 q_{iy} + c6_0 q_{iz}) + (c4_1 q_{ix} + c5_1 q_{iy} + c6_1 q_{iz})\Delta\phi + (c4_2 q_{ix} + c5_2 q_{iy} + c6_2 q_{iz})\Delta\theta + (c4_3 q_{ix} + c5_3 q_{iy} + c6_3 q_{iz})\Delta\psi \\ (c7_0 q_{ix} + c8_0 q_{iy} + c9_0 q_{iz}) + (c7_1 q_{ix} + c8_1 q_{iy} + c9_1 q_{iz})\Delta\phi + (c7_2 q_{ix} + c8_2 q_{iy} + c9_2 q_{iz})\Delta\theta + (c7_3 q_{ix} + c8_3 q_{iy} + c9_3 q_{iz})\Delta\psi \end{bmatrix}$$

$$= \mathbf{Q}_i \mathbf{e} + \mathbf{s}_i \tag{28}$$

where

$$\mathbf{Q}_i = \begin{bmatrix} cl_1 q_{ix} + c2_1 q_{iy} + c3_1 q_{iz} & cl_2 q_{ix} + c2_2 q_{iy} + c3_2 q_{iz} & cl_3 q_{ix} + c2_3 q_{iy} + c3_3 q_{iz} \\ c4_1 q_{ix} + c5_1 q_{iy} + c6_1 q_{iz} & c4_2 q_{ix} + c5_2 q_{iy} + c6_2 q_{iz} & c4_3 q_{ix} + c5_3 q_{iy} + c6_3 q_{iz} \\ c7_1 q_{ix} + c8_1 q_{iy} + c9_1 q_{iz} & c7_2 q_{ix} + c8_2 q_{iy} + c9_2 q_{iz} & c7_3 q_{ix} + c8_3 q_{iy} + c9_3 q_{iz} \end{bmatrix} \tag{29}$$

$$\mathbf{e} = \begin{bmatrix} \delta\phi \\ \delta\theta \\ \delta\psi \end{bmatrix} \tag{30}$$

$$\mathbf{s}_i = \begin{bmatrix} cl_0 q_{ix} + c2_0 q_{iy} + c3_0 q_{iz} \\ c4_0 q_{ix} + c5_0 q_{iy} + c6_0 q_{iz} \\ c7_0 q_{ix} + c8_0 q_{iy} + c9_0 q_{iz} \end{bmatrix} \tag{31}$$

Having derived $\mathbf{Q}_i$, $\mathbf{e}$, and $\mathbf{s}_i$, we obtain a new objective function similar to (17).

$$E(\mathbf{e}) = \mathbf{e}^T \mathbf{M} \mathbf{e} + 2\mathbf{m}^T \mathbf{e} + d \tag{32}$$

$$\text{where } \mathbf{M} = \sum_{i=1}^{n} \mathbf{G}_i^T \Lambda_i \mathbf{G}_i, \ \mathbf{m} = \sum_{i=1}^{n} \mathbf{G}_i^T \Lambda_i \mathbf{g}_i \text{ and } d = \sum_{i=1}^{n} \mathbf{g}_i^T \Lambda_i \mathbf{g}_i \tag{33}$$

Differentiating (32) with respect to $\mathbf{e}$ and setting it to zero yields

$$\nabla_{\mathbf{e}} E = 2\mathbf{M}\mathbf{e} + 2\mathbf{m} = \mathbf{0} \tag{34}$$

Rearranging Equation (34), we obtain the optimal solution

$$\mathbf{e}_{op} = -\mathbf{M}^{-1}\mathbf{m} \tag{35}$$

Once $\mathbf{e} = [\delta\phi, \delta\theta, \gamma\psi]^T$ is computed, we have the improved angle estimates,

$$\begin{bmatrix} \phi_{op} \\ \theta_{op} \\ \psi_{op} \end{bmatrix} = \begin{bmatrix} \phi_0 \\ \theta_0 \\ \psi_0 \end{bmatrix} + \begin{bmatrix} \delta\phi \\ \delta\theta \\ \delta\psi \end{bmatrix} \tag{36}$$

We construct $\mathbf{R}$ from these updated Euler angles, and compute the vehicle position as

$$\mathbf{p}_{robot} = -\mathbf{R}^T \mathbf{t}_{op} + \bar{\mathbf{p}} \tag{37}$$

The angle updates (35) and (36) are usually applied several times until no significant change occurs in e. In our applications, we found that no more than two iterations of (35) and (36) are needed to obtain the optimal solution.

2.4 Orthogonal Iteration (OI) Algorithm as Baseline

In this subsection, we present a pose estimation method known as the *orthogonal iteration* (OI), proposed by [6]. This method is also based on the collinearity property, and is shown to be efficient and robust. We will describe the formulation of this method, as it was used as a benchmark for performance comparison.

The objective is to minimise the following cost function

$$E(\mathbf{R},\mathbf{t}) = \sum_{i=1}^{n} \left\| \frac{\mathbf{R}\mathbf{q}_i + \mathbf{t}}{d_i} \right\|^2 - \left(\mathbf{v}_i^T \left[\frac{\mathbf{R}\mathbf{q}_i + \mathbf{t}}{d_i} \right] \right)^2, \tag{38}$$

which is identical to our cost function in Equation (2). The optimal translation vector, $\mathbf{t}$, is also obtained as

$$\mathbf{t}_{opt} = -\mathbf{\Lambda}^{-1} \sum_{i=1}^{n} \mathbf{\Lambda}_i \mathbf{R}\mathbf{q}_i \text{ where } \mathbf{\Lambda} = \sum_{i=1}^{n} \mathbf{\Lambda}_i \text{ and } \mathbf{\Lambda}_i = \frac{\mathbf{I} - \mathbf{V}_i}{d_i^2}. \tag{39}$$

Note that obtaining the actual value for $\mathbf{t}_{opt}$ requires the rotation matrix $\mathbf{R}$. This $\mathbf{R}$ can be obtained from the following algorithm known as the *absolute orientation* [1-2].

2.5 Absolute Orientation (AO)

Assuming that we have landmark position coordinates in both the body and reference frames, the absolute orientation algorithm finds $\mathbf{t}_{opt}$ and $\mathbf{R}$ which minimise the least-square error problem defined as below.

$$\text{Minimise } E(\mathbf{R},\mathbf{t}) = \sum_{i=1}^{n} \left\| \mathbf{R}\mathbf{q}_i + \mathbf{t} - \mathbf{r}_i \right\|^2 \text{ subject to } \mathbf{R}^T\mathbf{R} = \mathbf{I} \tag{40}$$

where $\mathbf{r}_i = d_i \mathbf{v}_i$.

Differentiating (40) with respect to $\mathbf{t}$, setting it to zero, and noting $\bar{\mathbf{q}} = \mathbf{0}$ yields

$$\mathbf{t}_{opt} = \frac{1}{n} \sum_{i=1}^{n} \left(-\mathbf{R}\mathbf{q}_i + \mathbf{r}_i \right) = -\mathbf{R}\bar{\mathbf{q}} + \bar{\mathbf{r}} = \bar{\mathbf{r}}. \tag{41}$$

Substituting (41) into (40) yields

$$\begin{aligned} E(\mathbf{R},\mathbf{t}) &= \sum_{i=1}^{n} \left\| \mathbf{R}\mathbf{q}_i - \mathbf{r}_i' \right\|^2 \text{ where } \mathbf{r}_i' = \mathbf{r}_i - \bar{\mathbf{r}}_i. \\ &= \sum_{i=1}^{n} \left(\mathbf{q}_i^T \mathbf{q}_i + \mathbf{r}_i'^T \mathbf{r}_i' - 2\mathbf{r}_i'^T \mathbf{R}\mathbf{q}_i \right). \end{aligned} \tag{42}$$

Our optimisation problem becomes maximising $\sum_{i=1}^{n} \mathbf{r}_i'^T \mathbf{R}\mathbf{q}_i$ subject to $\mathbf{R}^T\mathbf{R} = \mathbf{I}$. Since $\sum_{i=1}^{n} \mathbf{r}_i'^T \mathbf{R}\mathbf{q}_i$ is scalar, then

$$\begin{aligned}\sum_{i=1}^{n} \mathbf{r}_i'^T \mathbf{R}\mathbf{q}_i &= tr\left(\sum_{i=1}^{n} \mathbf{r}_i'^T \mathbf{R}\mathbf{q}_i\right) \\ &= tr\left(\sum_{i=1}^{n} \mathbf{R}\mathbf{q}_i \mathbf{r}_i'^T\right) \\ &= tr(\mathbf{RX}) \end{aligned} \tag{43}$$

where $\mathbf{X} = \sum_{i=1}^{n} \mathbf{q}_i \mathbf{r}_i'^T$ (44)

The trace becomes maximum when the matrix product $\mathbf{RX}$ is symmetric and positive definite. If we compute the SVD of $\mathbf{X}$ as $\mathbf{X} = \mathbf{U}\Sigma\mathbf{V}^T$ where $\mathbf{U}$ and $\mathbf{V}$ are orthogonal matrices and Σ is diagonal with non-negative elements, then $tr(\mathbf{RX})$ is maximised if

$$\mathbf{R} = \mathbf{V}\mathbf{U}^T \tag{45}$$

To prove this, we need to show that $\mathbf{RX} = \mathbf{V}\mathbf{U}^T(\mathbf{U}\Sigma\mathbf{V}^T)$ is symmetric and positive definite.

$$\begin{aligned}\mathbf{RX} &= \mathbf{V}\mathbf{U}^T(\mathbf{U}\Sigma\mathbf{V}^T) \\ &= \mathbf{V}\Sigma\mathbf{V}^T\end{aligned}$$

This is a symmetric matrix, and since the diagonal elements of Σ are non-negative, $\mathbf{RX}$ is positive definite. Note that one should make sure that the determinant of $\mathbf{R} = \mathbf{V}\mathbf{U}^T$ is 1.

The OI algorithm in [6] is implemented as follows:

1. Assume $\mathbf{r}_i = \mathbf{v}_i$ for $i = 1, \ldots, n$
2. compute $\mathbf{X} = \sum_{i=1}^{n} \mathbf{q}_i \mathbf{r}_i'^T$
3. $[\mathbf{U}, \Sigma, \mathbf{V}] = svd(\mathbf{X})$
4. $\mathbf{R}_{opt} = \mathbf{V}\mathbf{U}^T$ (initial $\mathbf{R}$ estimate for the next stage)
5. $\mathbf{t}_{opt} = -\mathbf{\Lambda}^{-1} \sum_{i=1}^{n} \mathbf{\Lambda}_i \mathbf{R}\mathbf{q}_i$
6. $d_i = \left\| \mathbf{R}_{opt}\mathbf{q}_i + \mathbf{t}_{opt} \right\|$ for $i = 1, \ldots, n$
7. $\mathbf{r}_i = d_i \mathbf{v}_i$ for $i = 1, \ldots, n$
8. Go to step 2 and repeat until $\mathbf{R}$ and $\mathbf{t}$ converge.

The vehicle position (in reference frame) is then obtained as $\bar{\mathbf{p}} - \mathbf{R}_{opt}^T \mathbf{t}_{opt}$. Steps 2-4 update the estimate of $\mathbf{R}$, which is then used to compute the translation vector in the fifth step.

We also look at a non-iterative method proposed by Lepetit, et al. [5] which is not based on the collinearity cost metric. This method expresses the 3D landmark points as a weighted sum of four control points and solves the problem in terms of their coordinates. The computer

simulations of this method indicate that this method is not as accurate and robust as the OI method. For fine-tuning, this method uses Gauss-Newton optimisation [1] which sometimes fails to converge if the measurements are noisy and the landmark number is small. Hence, we exclude this method in the performance comparison.

3. Simulations

3.1 Process Overview

The simulation process is outlined in Figure 4. The proposed method on the left side starts with initial azimuth estimation (AZIPE). Optionally, the AZIPE can also estimate the position if necessary. In the simulations, we start counting the iterations after the AZIPE. Likewise, the benchmark method runs the absolute orientation (AO) to come up with the initial attitude estimates before the iteration count-up starts.

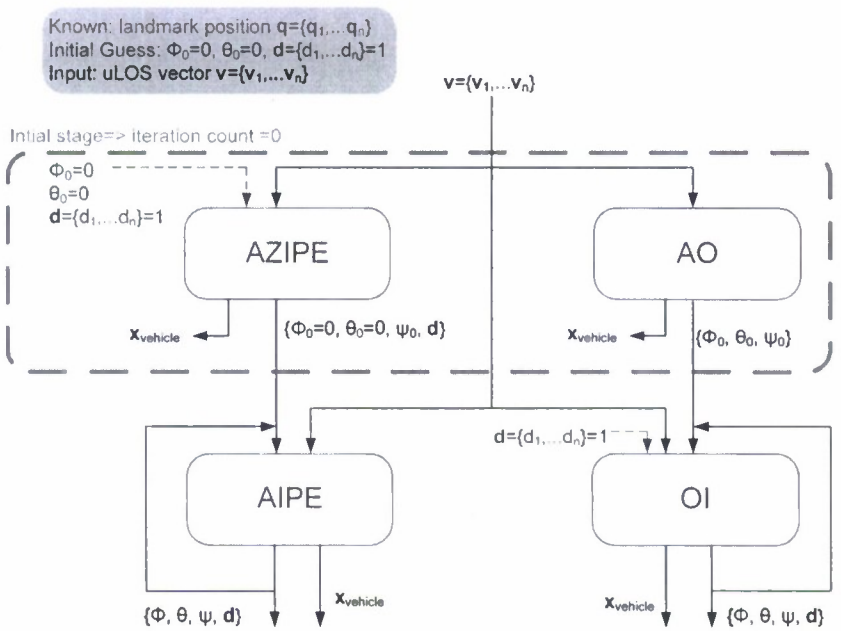

Figure 4: Process overview of the proposed method (left) and benchmark method (right)

We assume that the vehicle's tilt angles remain moderately small (eg., $\leq 40^\circ$), therefore assuming zero tilt angles for the AZIPE may be acceptable. On the other hand, the initial AO algorithm assumes $\mathbf{r}_i = \mathbf{v}_i$ (i.e., all the landmarks are unit distance away from the vehicle). The role of the initial estimator is to bring the initial estimate close to the global minimum, so the global convergence is ensured when the AIPE or OI is executed.

The AIPE and OI were run iteratively, gradually improving the attitude and position estimates by feeding back the attitude and vehicle/landmark distance estimates. Steps 2-4 in Section 2.4 are run to produce the initial **R** estimate required by the fifth step. Steps 5-7 followed by steps 2-4 (i.e., AO) form the OI process.

The following are the default parameter settings for the simulations. The parameters remain unchanged except for the one whose effect we want to see on the system performance. These are

- $\sigma(\theta_{el}) = 3^\circ$ and $\sigma(\theta_{az}) = 3^\circ$ for each AOA measurements.
- Landmark positions: {(0, 0, -10), (40, 0, -10), (0, 40, -10), (40, 40, -10)} {(0, 20, -10), (20, 0, -10), (20, 40, -10), (40, 20, -10)}m (negative z => positive altitude)
- Vehicle orientation: $[\phi, \theta, \psi] = [20^\circ, 20^\circ, 45^\circ]$
- Vehicle position: $[x, y, z]$=[4m, 10m, 0m]
- Number of iterations=4.

In the following subsections, we conduct 1000 Monte-Carlo simulations to generate the performance metric in terms of estimation error statistics. It is expressed as the root mean square (RMS) of the horizontal-position, height, tilt and azimuth errors. We define the horizontal position and tilt errors as $\sqrt{x_{err}^2 + y_{err}^2}$ and $\sqrt{\phi_{err}^2 + \theta_{err}^2}$ respectively. The error curves from the proposed and benchmark methods will be shown in green and blue respectively, and will be compared with the Cramer-Rao Lower Bound (CRLB) shown in red.

The CRLB represents the smallest estimation error (RMS) that any unbiased method can possibly achieve for the given geometry and measurement errors. We assume that the measurement errors are Gaussian of mean zero. The descriptive derivation of the CRLB is given in Appendix D.

3.2 Convergence Speed

In this subsection, we examine the convergence trend of both localisation methods. The iteration-count up to 10 is attempted and the results are given in Figure 5. Zero iteration means that the process stopped after the initial stage. For index of zero, the horizontal position error of the AO is much larger than that of the AZIPE, whereas the other error terms from the two methods are comparable. Both methods converge rapidly: 3-4 iterations for the OI and 2 iterations for the AIPE. It appears that the small angle approximations in the AIPE tolerate the initial roll and pitch errors of $(20^\circ, 20^\circ)$ and azimuth error of 7° (σ)

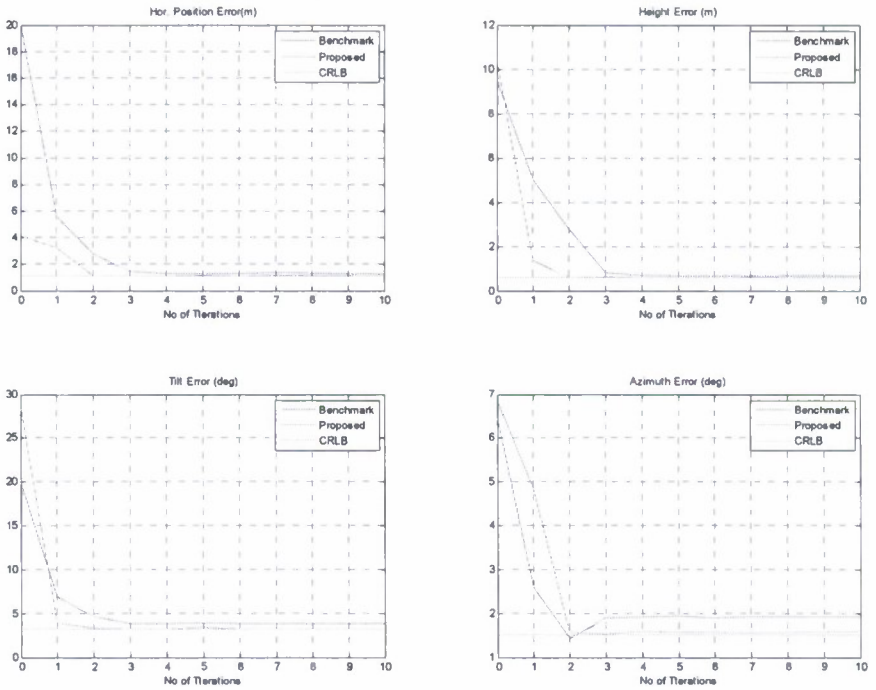

Figure 5: Estimation Error versus number of iterations at default location (4,10,0)

Apart from the convergence speed, the AIPE is also favoured in terms of post convergence residual errors. It is noticed that the error differences are more evident for angular terms than for the positional terms. Such differences between the two methods arise from the fact that the objective function used in the AO (see Equation (40)) is not always a close approximation of true collinearity measure. The weights are not equally distributed to the landmarks - more weights are given to the far landmarks than to the near landmarks. The AO would perform better if the landmarks are equally distant from the vehicle.

To demonstrate this, we ran another simulation where the vehicle is moved to (20,20,0) m so that the distances to all the landmarks are similar. The new estimation errors are given in

Figure 6. With the new geometric arrangement, the AO algorithm produces a very accurate initial pose estimate, which gets slightly worse as the OI iteration takes place. The OI solutions converge after 1-2 iterations, and the attitude accuracy is significantly closer to that of the AIPE. The AIPE converges after 2 iterations as before, showing convergence patterns that are more consistent regardless of the geometric changes. For the remaining simulations, we apply a fixed iteration-count of 4 to the two methods.

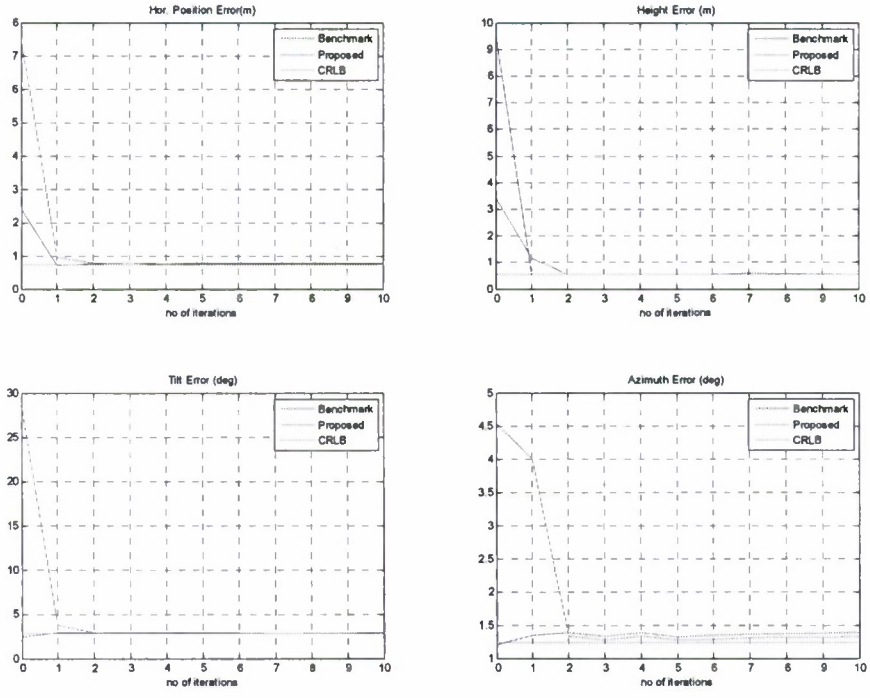

Figure 6: Estimation errors versus number of iterations at another location (20, 20, 0). Initial AO algorithm of the benchmark method works better as the distances from the vehicle to the landmarks are similar.

3.3 Effect of Measurement Errors

Here we explore the effect of the measurement (AOA) errors on the estimation accuracy. The elevation and azimuth errors (σ) are equally varied from 0.1° to 10°, and the results are shown in Figure 7. The green curves (proposed) remain closer to the CRLB curve (red) than the blue curves (benchmark) do, within the entire angle error range.

It is noticed that the green curves start to depart from the red curves when the AOA angle exceeds 3°. To explain this we revisit Equation (4)

$$E(\mathbf{R},\mathbf{t}) = \sum_{i=1}^{n} \left\| \frac{\mathbf{R}\mathbf{q}_i + \mathbf{t}}{d_i} \right\|^2 - \left(\mathbf{v}_i^T \left[\frac{\mathbf{R}\mathbf{q}_i + \mathbf{t}}{d_i} \right] \right)^2 .$$

According to the diagram in Figure 3, we realise that

$$\left\| \frac{\mathbf{R}\mathbf{q}_i + \mathbf{t}}{d_i} \right\|^2 - \left(\mathbf{v}_i^T \left[\frac{\mathbf{R}\mathbf{q}_i + \mathbf{t}}{d_i} \right] \right)^2 = \left(\sin(AOA\_err)\right)^2 .$$

For small AOA errors (eg., $\leq 3^\circ$), the following approximation holds:

$\sin(AoA\_err) \approx AOA\_err$.

Therefore, for small AOA errors, the cost function can be expressed as

$E(\mathbf{R},\mathbf{t}) \approx \sum_{i=1}^{n} (AOA\_err)^2$, which is the same as the cost function associated with the CRLB.

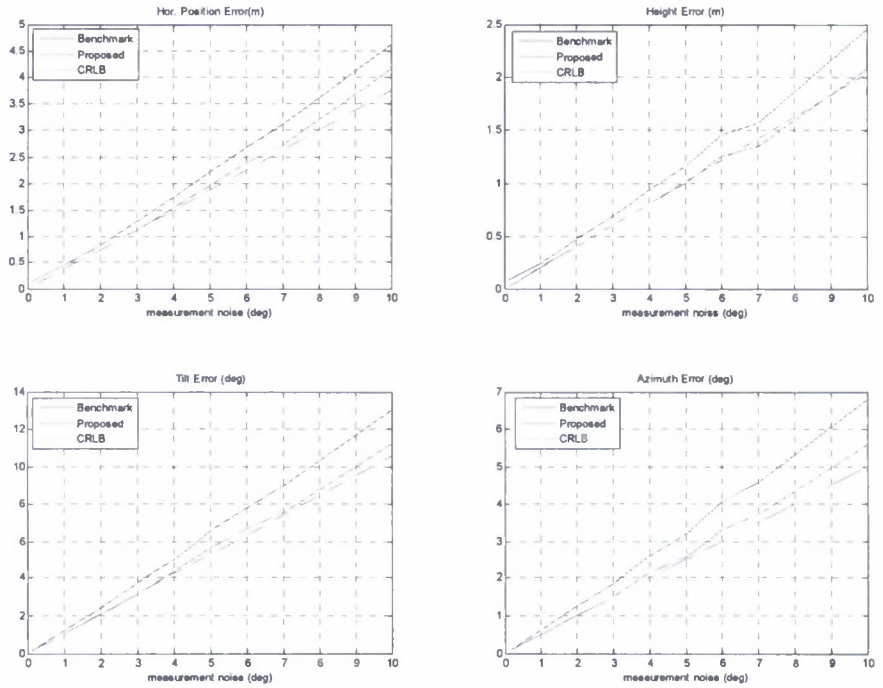

Figure 7: Estimation errors versus AOA noise

3.4 Effect of Initial Tilt Error

In Section 3.2, we observed that the AZIPE produced a large azimuth error of 7° when the initial tilt error was 20°. If the initial tilt error is larger, then the azimuth error will be even larger placing the initial estimate far from the global minimum. Here we examine if the AIPE and OI are capable of consistently steering the estimate towards the global minimum.

Figure 8 shows no sign of divergence – the blue and red curves follow the shape of the red curves. The shape variation of the curves is mainly due to the fact that the AOA measurements change when the vehicle tilt changes. For example, the landmarks in the left and right of the vehicle with zero tilt, will appear above and below when the vehicle rolls 90°. Such measurement changes alter the cost function leading to the variations in all three curves in Figure 8. It appears that the proposed and the benchmark methods are capable of consistently bringing the coarse initial estimate to global minimum. Again, the proposed method produces more accurate estimates than the benchmark.

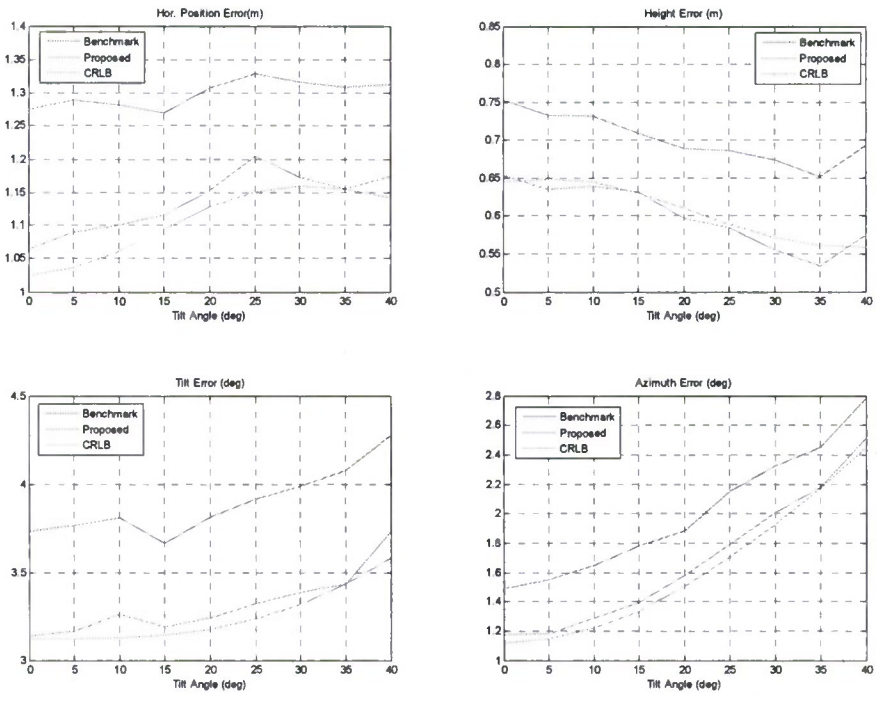

Figure 8 Estimation errors versus the vehicle tilt angles. Tilt angles are applied equally to the roll and pitch.

3.5 Effect of Landmark Numbers

In this subsection, we look at the effect of landmark numbers (n) on the estimation accuracy. The landmark number is varied from n=4 to 16 in steps of 2. The 16 landmark locations are given in Appendix E.

As in Figure 9, the localisation errors clearly decrease as n increases. The error reductions for the attitude are more gradual and the pattern seems to continue past n=16. On the other hand, for the position, the error reductions are more abrupt for n=4~6, and become slower for the larger n.

As expected, increasing the number of landmarks improves the estimation accuracy, however this also increases the computational effort ($O(n)$). Again, the proposed method outperforms the benchmark method.

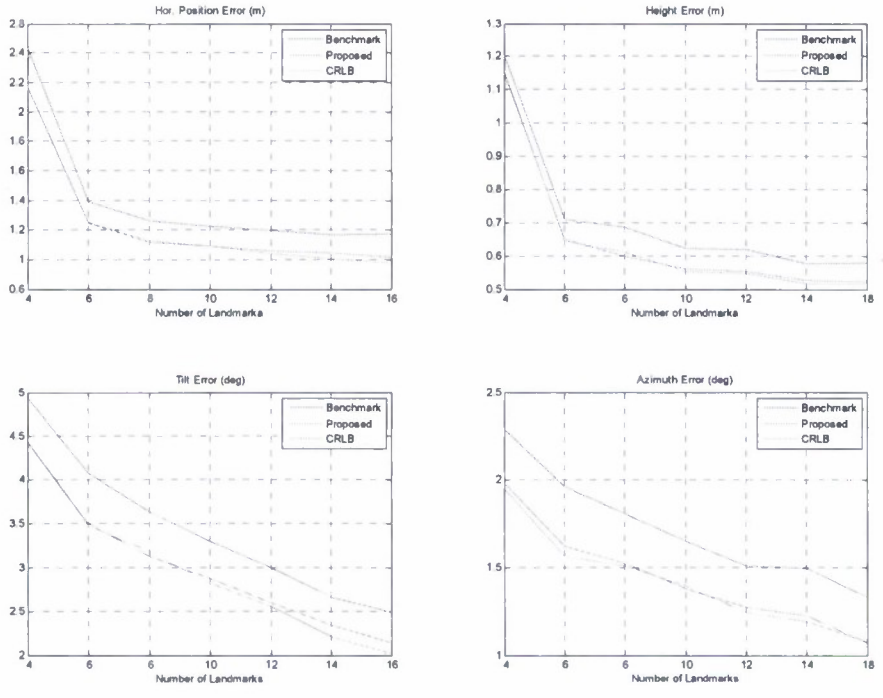

Figure 9 Estimation errors versus number of landmarks.

3.6 Random Positions and Orientations

In this subsection, we randomise the vehicle position/orientation and the landmark positions. Both the vehicle and landmark positions are uniformly distributed within [-20 20] for all three axes. The vehicle roll and pitch angles are uniformly distributed within [-40° 40°] and the azimuth angle has an uniform distribution within [-180° 180°]. The aim is to try exhaustive combinations of geometries and see if the proposed method is consistently better than the OI method. In this test, we try five levels of difficulties, where the difficult setting has a smaller number of very noisy measurements and the easy setting has a large number of less noisy measurements (see Table 1).

Table 1: Five difficulty indices and the associated measurement arrangements

Difficulty Index	1	2	3	4	5
Landmark Numbers	8	12	16	20	24
Measurement Noise	5	4	3	2	1

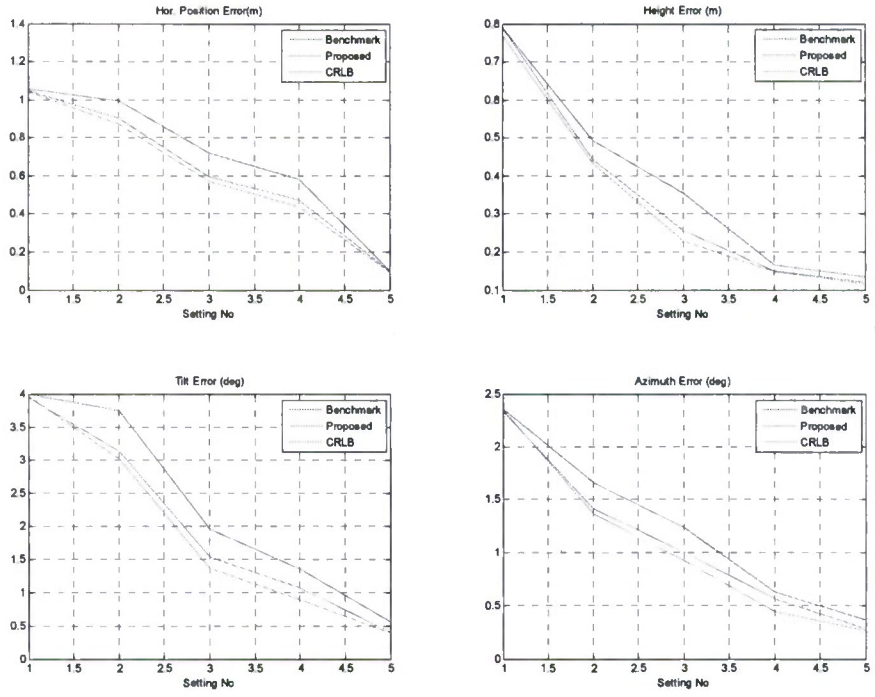

Figure 10: Estimation errors versus difficulty indices, when the vehicle-landmark geometries are made random. Higher the index, easier the problem.

Figure 10 shows the RMS errors after 3000 Monte-Carlo simulations. All the errors terms decrease as the number of measurements increases and the measurement noise decreases. It is also clear that the proposed method consistently outperforms the OI method, reinforcing the previous findings.

4. Conclusions

In this study, we present an accurate and efficient 3D localisation method that uses the angle of arrival measurements from stationary landmarks. The underlying idea is to minimise the collinearity error between the measured and estimated uLOS vectors. The algorithm runs in two parts - the AZIPE for initial azimuth estimation assuming zero tilt and the AIPE for progressively improving all three orientation angles. The findings from the experiments are:

- The proposed algorithm converges fast (e.g., <3 iterations) for general geometric configurations.
- The proposed algorithm tolerates large measurement and tilt errors.
- The estimation accuracy improves as the number of landmarks increases. However, the computation effort also increases as the number of landmark increases ($\sim O(n)$).
- In all cases, the proposed method outperforms the benchmark method.

The proposed method appears to be accurate, globally convergent and computationally efficient requiring only a small number of iterations.

5. References

1. Dougancay, K., and Ibal, G., "*3D Passive Bearing-Only Emitter Localisation Using Crude Angle-of-Arrival Measurements*", Proceedings of Tenth SimTech, May, 2005.
2. Horn, B.K.P, "*Closed-Form Solution of Absolution Orientation Using Unit Qaternion,*" J. Optical Soc. Am., Vol. 4, 1987, pp. 629-642.
3. Horn, B.K.P, Hilden, H.M., and Negahdaripour, S., "*Closed-form Solution of Absolution Orientation using Orthonormal Matrices*", J. Optical Soc. Am., Vol. 5, 1988, pp. 1127-1135.
4. Kim, J. and Hmam, H., "*Landmark Based Navigation of Unmanned Ground Vehicle*", DSTO_TR_2260, 2009.
5. Lepetit, V., Moreno-Noguer, F., and Fua, P.,"*EPnP: An Accurate O(n) Solution to the PnP Problem*", International Journal of Computer Vision, 2008.
6. Lu, C., Hager, G.D., and Mjolsness, E., "*Fast and Globally Convergent Pose Estimation from Video Images*", IEEE Transactions on Pattern Analysis and Machine Intelligence, Vol. 22, No. 6, June 2000, pp 610-622.
7. Torrieri, D.J., "*Statistical Theory of Passive Location Systems*", IEEE Transactions on Aerospace and Electronic Systems, Vol. AES-20, No. 2, March 1984, pg 183-198.

THIS PAGE HAS BEEN
INTENTIONALLY
LEFT BLANK

Appendix A: Derivation of Optimal Translation

Given

$$E(\mathbf{R},\mathbf{t}) = \sum_{i=1}^{n} \left\| \frac{\mathbf{R}\mathbf{q}_i + \mathbf{t}}{d_i} \right\|^2 - \left(\mathbf{v}_i^T \left[\frac{\mathbf{R}\mathbf{q}_i + \mathbf{t}}{d_i} \right] \right)^2 \tag{A1}$$

If we let $\mathbf{V}_i = \mathbf{v}_i \mathbf{v}_i^T$ then the optimal translation vector, $\mathbf{t}$, is given by

$$\begin{aligned}
E(\mathbf{R},\mathbf{t}) &= \sum_{i=1}^{n} \left[\frac{\mathbf{R}\mathbf{q}_i + \mathbf{t}}{d_i} \right]^T \left[\frac{\mathbf{R}\mathbf{q}_i + \mathbf{t}}{d_i} \right] - \mathbf{v}_i^T \left[\frac{\mathbf{R}\mathbf{q}_i + \mathbf{t}}{d_i} \right] \mathbf{v}_i^T \left[\frac{\mathbf{R}\mathbf{q}_i + \mathbf{t}}{d_i} \right] \\
&= \sum_{i=1}^{n} \frac{1}{d_i^2} \left(\mathbf{q}_i^T \mathbf{R}^T + \mathbf{t}^T \right) \left(\mathbf{R}\mathbf{q}_i + \mathbf{t} \right) - \frac{1}{d_i^2} \left(\mathbf{v}_i^T \mathbf{R}\mathbf{q}_i - \mathbf{v}_i^T \mathbf{t} \right) \left(\mathbf{v}_i^T \mathbf{R}\mathbf{q}_i - \mathbf{v}_i^T \mathbf{t} \right) \\
&= \sum_{i=1}^{n} \frac{1}{d_i^2} \left\{ \mathbf{q}_i^T \mathbf{R}^T \mathbf{R}\mathbf{q}_i + \mathbf{q}_i^T \mathbf{R}^T \mathbf{t} + \mathbf{t}^T \mathbf{R}\mathbf{q}_i + \mathbf{t}^T \mathbf{t} - \left(\mathbf{q}_i^T \mathbf{R}^T \mathbf{v}_i - \mathbf{t}^T \mathbf{v}_i \right) \left(\mathbf{v}_i^T \mathbf{R}\mathbf{q}_i - \mathbf{v}_i^T \mathbf{t} \right) \right\} \\
&= \sum_{i=1}^{n} \frac{1}{d_i^2} \left\{ \mathbf{q}_i^T \mathbf{q}_i + 2\mathbf{q}_i^T \mathbf{R}^T \mathbf{t} + \mathbf{t}^T \mathbf{t} - \left(\mathbf{q}_i^T \mathbf{R}^T \mathbf{v}_i \mathbf{v}_i^T \mathbf{R}\mathbf{q}_i - \mathbf{q}_i^T \mathbf{R}^T \mathbf{v}_i \mathbf{v}_i^T \mathbf{t} - \mathbf{t}^T \mathbf{v}_i \mathbf{v}_i^T \mathbf{R}\mathbf{q}_i + \mathbf{t}^T \mathbf{v}_i \mathbf{v}_i^T \mathbf{t} \right) \right\} \\
&= \sum_{i=1}^{n} \frac{1}{d_i^2} \left\{ \mathbf{q}_i^T \mathbf{q}_i + 2\mathbf{t}^T \mathbf{R}\mathbf{q}_i + \mathbf{t}^T \mathbf{t} - \left(\mathbf{q}_i^T \mathbf{R}^T \mathbf{V}_i \mathbf{R}\mathbf{q}_i - \mathbf{q}_i^T \mathbf{R}^T \mathbf{V}_i \mathbf{t} - \mathbf{t}^T \mathbf{V}_i \mathbf{R}\mathbf{q}_i + \mathbf{t}^T \mathbf{V}_i \mathbf{t} \right) \right\} \\
&= \sum_{i=1}^{n} \frac{1}{d_i^2} \left\{ \mathbf{t}^T (\mathbf{I} - \mathbf{V}_i)\mathbf{t} + 2\mathbf{t}^T (\mathbf{I} - \mathbf{V}_i)\mathbf{R}\mathbf{q}_i - \mathbf{q}_i^T \mathbf{R}^T \mathbf{V}_i \mathbf{R}\mathbf{q}_i + \mathbf{q}_i^T \mathbf{q}_i \right\}
\end{aligned} \tag{A2}$$

Let $\mathbf{\Lambda}_i = \frac{(\mathbf{I} - \mathbf{V}_i)}{d_i^2}$, then setting $\frac{\partial E(\mathbf{R},\mathbf{t})}{\partial \mathbf{t}}$ to zero gives

$$\frac{\partial E(\mathbf{R},\mathbf{t})}{\partial \mathbf{t}} = \sum_{i=1}^{n} \frac{1}{d_i^2} \left\{ 2(\mathbf{I} - \mathbf{V}_i)\mathbf{t} + 2(\mathbf{I} - \mathbf{V}_i)\mathbf{R}\mathbf{q}_i \right\} = 0$$

$$\sum_{i=1}^{n} \frac{1}{d_i^2} (\mathbf{I} - \mathbf{V}_i)\mathbf{t} + \frac{1}{d_i^2} (\mathbf{I} - \mathbf{V}_i)\mathbf{R}\mathbf{q}_i = 0$$

$$\left(\sum_{i=1}^{n} \mathbf{\Lambda}_i \right) \mathbf{t} + \sum_{i=1}^{n} \mathbf{\Lambda}_i \mathbf{R}\mathbf{q}_i = 0$$

and therefore

$$\mathbf{t}_{opt}(\mathbf{R}) = -\mathbf{\Lambda}^{-1} \sum_{i=1}^{n} \mathbf{\Lambda}_i \mathbf{R}\mathbf{q}_i \quad \text{where } \mathbf{\Lambda} = \sum_{i=1}^{n} \mathbf{\Lambda}_i \tag{A3}$$

THIS PAGE HAS BEEN
INTENTIONALLY
LEFT BLANK

Appendix B: Derivation of Quadratic Cost Function

$$E(\mathbf{R},\mathbf{t}) = \sum_{i=1}^{n} \left\| \frac{\mathbf{R}\mathbf{q}_i + \mathbf{t}}{d_i} \right\|^2 - \left(\mathbf{v}_i^T \left[\frac{\mathbf{R}\mathbf{q}_i + \mathbf{t}}{d_i} \right] \right)^2 \tag{B1}$$

Replacing $\mathbf{R}\mathbf{q}_i + \mathbf{t}$ with $\mathbf{G}_i\mathbf{e} + \mathbf{g}_i$ gives:

$$\begin{aligned}
E(\mathbf{e}) &= \sum_{i=1}^{n} \left\| \frac{\mathbf{G}_i\mathbf{e} + \mathbf{g}_i}{d_i} \right\|^2 - \left(\frac{\mathbf{v}_i^T(\mathbf{G}_i\mathbf{e} + \mathbf{g}_i)}{d_i} \right)^2 \\
&= \sum_{i=1}^{n} \frac{\mathbf{e}^T\mathbf{G}_i^T\mathbf{G}_i\mathbf{e} + \mathbf{g}_i{}^T\mathbf{g}_i + 2\mathbf{g}_i{}^T\mathbf{G}_i\mathbf{e}}{d_i^2} - \frac{\mathbf{e}^T\mathbf{G}_i^T\mathbf{v}_i\mathbf{v}_i^T\mathbf{G}_i\mathbf{e} + \mathbf{g}_i{}^T\mathbf{v}_i\mathbf{v}_i^T\mathbf{g}_i + 2\mathbf{g}_i{}^T\mathbf{v}_i\mathbf{v}_i^T\mathbf{G}_i\mathbf{e}}{d_i^2} \\
&= \sum_{i=1}^{n} \frac{\mathbf{e}^T\mathbf{G}_i^T(\mathbf{I} - \mathbf{V}_i)\mathbf{G}_i\mathbf{e} + 2\mathbf{g}_i{}^T(\mathbf{I} - \mathbf{V}_i)\mathbf{G}_i\mathbf{e} + \mathbf{g}_i{}^T(\mathbf{I} - \mathbf{V}_i)\mathbf{g}_i}{d_i^2} \\
&= \sum_{i=1}^{n} \mathbf{e}^T\mathbf{G}_i^T\boldsymbol{\Lambda}_i\mathbf{G}_i\mathbf{e} + 2\mathbf{g}_i{}^T\boldsymbol{\Lambda}_i\mathbf{G}_i\mathbf{e} + \mathbf{g}_i{}^T\boldsymbol{\Lambda}_i\mathbf{g}_i \\
&= \mathbf{e}^T\left(\sum_{i=1}^{n} \mathbf{G}_i^T\boldsymbol{\Lambda}_i\mathbf{G}_i \right)\mathbf{e} + 2\left(\sum_{i=1}^{n} \mathbf{g}_i{}^T\boldsymbol{\Lambda}_i\mathbf{G}_i \right)\mathbf{e} + \sum_{i=1}^{n} \mathbf{g}_i{}^T\boldsymbol{\Lambda}_i\mathbf{g}_i
\end{aligned} \tag{B2}$$

$$E(\mathbf{e}) = \mathbf{e}^T\mathbf{M}\mathbf{e} + 2\mathbf{m}^T\mathbf{e} + d \tag{B3}$$

THIS PAGE HAS BEEN
INTENTIONALLY
LEFT BLANK

Appendix C: Linearised Rotation Matrix

$$\mathbf{R} \cong \begin{bmatrix} c1 & c2 & c3 \\ c4 & c5 & c6 \\ c7 & c8 & c9 \end{bmatrix}$$

where

$$\begin{aligned} c1 &= \cos\theta\cos\psi_0 && \textbf{in the form of } c1 = c1_0 \\ &\quad +(0)\delta\phi && \quad +c1_1\delta\phi \\ &\quad -(\sin\theta_0\cos\psi_0)\delta\theta && \quad +c1_2\delta\theta \\ &\quad -(\cos\theta_0\sin\psi_0)\delta\psi && \quad +c1_3\delta\psi \end{aligned} \tag{C1}$$

$$\begin{aligned} c2 &= \cos\theta_0\sin\psi_0 \\ &\quad +(0)\delta\phi \\ &\quad -(\sin\theta_0\sin\psi_0)\delta\theta \\ &\quad +(\cos\theta_0\cos\psi_0)\delta\psi \end{aligned} \tag{C2}$$

$$\begin{aligned} c3 &= -\sin\theta_0 \\ &\quad +(0)\delta\phi \\ &\quad -(\cos\theta_0)\delta\theta \\ &\quad +(0)\delta\psi \end{aligned} \tag{C3}$$

$$\begin{aligned} c4 &= (\sin\phi_0\sin\theta_0\cos\psi_0 - \cos\phi_0\sin\psi_0) \\ &\quad +(\cos\phi_0\sin\theta_0\cos\psi_0 + \sin\phi_0\sin\psi_0)\delta\phi \\ &\quad +(\sin\phi_0\cos\theta_0\cos\psi_0)\delta\theta \\ &\quad +(\cos\phi_0\cos\psi_0 - \sin\theta_0\sin\phi_0\sin\psi_0)\delta\psi \end{aligned} \tag{C4}$$

$$\begin{aligned} c5 &= (\sin\phi_0\sin\theta_0\sin\psi_0 + \cos\phi_0\cos\psi_0) \\ &\quad +(\cos\phi_0\sin\theta_0\sin\psi_0 - \sin\phi_0\cos\psi_0)\delta\phi \\ &\quad +(\sin\phi_0\cos\theta_0\sin\psi_0)\delta\theta \\ &\quad +(-\cos\phi_0\sin\psi_0 + \sin\phi_0\sin\theta_0\cos\psi_0)\delta\psi \end{aligned} \tag{C5}$$

$$\begin{aligned} c6 &= \sin\phi_0\cos\theta_0 \\ &\quad +(\cos\phi_0\cos\theta_0)\delta\phi \\ &\quad -(\sin\phi_0\sin\theta_0)\delta\theta \\ &\quad +(0)\delta\psi \end{aligned} \tag{C6}$$

$$
\begin{aligned}
c7 = {} & (\cos\phi_0 \sin\theta_0 \cos\psi_0 + \sin\phi_0 \sin\psi_0) \\
& + (-\sin\phi_0 \sin\theta_0 \cos\psi_0 + \cos\phi_0 \sin\psi_0)\delta\phi \\
& + (\cos\phi_0 \cos\theta_0 \cos\psi_0)\delta\theta \\
& + (\sin\phi_0 \cos\psi_0 - \cos\phi_0 \sin\theta_0 \sin\psi_0)\delta\psi
\end{aligned} \tag{C7}
$$

$$
\begin{aligned}
c8 = {} & (\cos\phi_0 \sin\theta_0 \sin\psi_0 - \sin\phi_0 \cos\psi_0) \\
& + (-\sin\phi_0 \sin\theta_0 \sin\psi_0 - \cos\phi_0 \cos\psi_0)\delta\phi \\
& + (\cos\phi_0 \cos\theta_0 \sin\psi_0)\delta\theta \\
& + (\sin\phi_0 \sin\psi_0 + \cos\phi_0 \sin\theta_0 \cos\psi_0)\delta\psi
\end{aligned} \tag{C8}
$$

$$
\begin{aligned}
c9 = {} & \cos\phi_0 \cos\theta_0 \\
& - (\sin\phi_0 \cos\theta_0)\delta\phi \\
& - (\cos\phi_0 \sin\theta_0)\delta\theta \\
& + (0)\delta\psi
\end{aligned} \tag{C9}
$$

Appendix D: Derivation of CRLB

The Maximum Likelihood Estimator (MLE) [1][7] has the following objective function:

$$\text{Minimise } E(\mathbf{x}) = \sum_{i=1}^{n} \begin{bmatrix} \alpha_i - f_{\alpha_i}(\hat{\mathbf{x}}) & \beta_i - f_{\beta_i}(\hat{\mathbf{x}}) \end{bmatrix} \cdot \mathbf{N}_i^{-1} \cdot \begin{bmatrix} \alpha_i - f_{\alpha_i}(\hat{\mathbf{x}}) \\ \beta_i - f_{\beta_i}(\hat{\mathbf{x}}) \end{bmatrix} \tag{D1}$$

where

$\mathbf{x} = [x \quad y \quad z \quad \phi \quad \theta \quad \psi]^T$: vehicle position and orientation,

$\mathbf{N}_i = \begin{bmatrix} \sigma_{\alpha_i}^2 & 0 \\ 0 & \sigma_{\beta_i}^2 \end{bmatrix}$: covariance matrix for i^{th} elevation (α) and azimuth (β) measurements,

$f_{\alpha_i}(\hat{\mathbf{x}}) = \tan^{-1}\left(\frac{\mathbf{v}_i(2)}{\mathbf{v}_i(1)}\right)$, $f_{\beta_i}(\hat{\mathbf{x}}) = \tan^{-1}\left(\frac{-\mathbf{v}_i(3)}{\sqrt{\mathbf{v}_i(1)^2 + \mathbf{v}_i(2)^2}}\right)$ and $\mathbf{v}_i = \mathbf{R}(\mathbf{p}_i - [x, y, z]^T)$.

The elevation and azimuth functions $f_{\alpha_i}(\hat{\mathbf{x}})$ and $f_{\beta_i}(\hat{\mathbf{x}})$ are non-linear (contains trigonometric terms). Omitting $(\hat{\mathbf{x}})$ from the functions, we define the Jacobian matrix for the i^{th} landmark as

$$\mathbf{F}_i = \begin{bmatrix} \frac{\partial f_{\alpha_i}}{\partial x} & \frac{\partial f_{\alpha_i}}{\partial y} & \frac{\partial f_{\alpha_i}}{\partial z} & \frac{\partial f_{\alpha_i}}{\partial \phi} & \frac{\partial f_{\alpha_i}}{\partial \theta} & \frac{\partial f_{\alpha_i}}{\partial \psi} \\ \frac{\partial f_{\beta_i}}{\partial x} & \frac{\partial f_{\beta_i}}{\partial y} & \frac{\partial f_{\beta_i}}{\partial z} & \frac{\partial f_{\beta_i}}{\partial \phi} & \frac{\partial f_{\beta_i}}{\partial \theta} & \frac{\partial f_{\beta_i}}{\partial \psi} \end{bmatrix}. \tag{D2}$$

Vertically cascading for all the landmarks, we get

$$\mathbf{F} = \begin{bmatrix} \mathbf{F}_1 \\ \vdots \\ \mathbf{F}_n \end{bmatrix} \text{ and } \mathbf{N} = \begin{bmatrix} \mathbf{N}_1 & \mathbf{0} & \mathbf{0} \\ \mathbf{0} & \ddots & \mathbf{0} \\ \mathbf{0} & \mathbf{0} & \mathbf{N}_n \end{bmatrix} \tag{D3}$$

The error covariance matrix for $\hat{\mathbf{x}}$ is given as

$$\mathbf{P} = (\mathbf{F}^{-1}\mathbf{N}^{-1}\mathbf{F})^{-1} \tag{D4}$$

And the square root of its diagonal elements are the CLRBs for the six parameters, $(x, y, z, \phi, \theta, \psi)$.

THIS PAGE HAS BEEN
INTENTIONALLY
LEFT BLANK

Appendix E: Landmark Locations

Total of 16 landmarks are available, and the first n landmarks are chosen in the simulations. For example, if n=6 then $\mathbf{p}_1$ to $\mathbf{p}_6$ are selected. Note that negative z means positive height.

P_1	=	(0, 0, -10)	m
P_2	=	(40, 0, -10)	m
P_3	=	(0, 40, -10)	m
P_4	=	(40, 40, -10)	m
P_5	=	(0, 20, -10)	m
P_6	=	(20, 0, -10)	m
P_7	=	(40, 20, -10)	m
P_8	=	(20, 40, -10)	m
P_9	=	(0, 0, -20)	m
P_{10}	=	(40, 0, -20)	m
P_{11}	=	(0, 40, -20)	m
P_{12}	=	(40, 40, -20)	m
P_{13}	=	(0, 0, -40)	m
P_{14}	=	(40, 0, -40)	m
P_{15}	=	(0, 40, -40)	m
P_{16}	=	(40, 40, -40)	m

DEFENCE SCIENCE AND TECHNOLOGY ORGANISATION DOCUMENT CONTROL DATA	1. PRIVACY MARKING/CAVEAT (OF DOCUMENT)

2. TITLE	3. SECURITY CLASSIFICATION (FOR UNCLASSIFIED REPORTS THAT ARE LIMITED RELEASE USE (L) NEXT TO DOCUMENT CLASSIFICATION)
3D Self-Localisation from Angle of Arrival Measurements	Document (U) Title (U) Abstract (U)
4. AUTHOR(S)	5. CORPORATE AUTHOR
Jijoong Kim and Hatem Hmam	DSTO Defence Science and Technology Organisation PO Box 1500 Edinburgh South Australia 5111 Australia

6a. DSTO NUMBER	6b. AR NUMBER	6c. TYPE OF REPORT	7. DOCUMENT DATE
DSTO-TR-2278	AR-014-502	Technical Report	April 2009

8. FILE NUMBER	9. TASK NUMBER	10. TASK SPONSOR	11. NO. OF PAGES	12. NO. OF REFERENCES
2008/1127664	07/249	CWSD	29	7

13. URL on the World Wide Web	14. RELEASE AUTHORITY
http://www.dsto.defence.gov.au/corporate/reports/DSTO-TR-2278.pdf	Chief, Weapons Systems Division

15. SECONDARY RELEASE STATEMENT OF THIS DOCUMENT

Approved for public release

OVERSEAS ENQUIRIES OUTSIDE STATED LIMITATIONS SHOULD BE REFERRED THROUGH DOCUMENT EXCHANGE, PO BOX 1500, EDINBURGH, SA 5111

16. DELIBERATE ANNOUNCEMENT

No Limitations

17. CITATION IN OTHER DOCUMENTS Yes

18. DSTO RESEARCH LIBRARY THESAURUS http://web-vic.dsto.defence.gov.au/workareas/library/resources/dsto_thesaurus.shtml

Localisation, Optimisation, Collinearity

19. ABSTRACT

We propose a 3D self-localisation method that uses 3D angle of arrival (AOA) information (ie., azimuth and elevation measurements) from landmarks. The formulation is based on minimising the collinearity error between the estimated line of sight (LOS) to the landmark and the measured AOA. This method runs in two parts - initial estimation of the vehicle azimuth and position assuming the vehicle has no tilt, and iterative 3D pose estimation based on a small angle approximation approach. Simulation study indicates that this method is efficient, requiring a small number of iterations, globally convergent and robust.